# Relaxation-weighted [23]Na magnetic resonance imaging maps regional patterns of abnormal sodium concentrations in amyotrophic lateral sclerosis

Hans-Peter Müller*, Armin M. Nagel*(iD), Franziska Keidel, Arthur Wunderlich, Annemarie Hübers (iD), Lena V. Gast, Albert C. Ludolph, Meinrad Beer† and Jan Kassubek† (iD)

## Abstract

**Objectives:** Multiparametric magnetic resonance imaging (MRI) is established as a technical instrument for the characterisation of patients with amyotrophic lateral sclerosis (ALS). The contribution of relaxation-weighted sodium ([23]NaR) MRI remains to be defined. The aim of this study is to apply [23]NaR MRI to investigate brain sodium homeostasis and map potential alterations in patients with ALS as compared with healthy controls.

**Materials and Methods:** Seventeen patients with ALS (mean age $61.1 \pm 11.4$ years, m/f = 9/8) and 10 healthy control subjects (mean age $60.3 \pm 15.3$ years, m/f = 6/4) were examined by [23]NaR MRI at 3 T. Regional sodium maps were obtained by the calculation of the weighted difference from two image data sets with different echo times ($TE_1 = 0.3$ ms, $TE_2 = 25$ ms). Voxel-based analysis of the relaxation-weighted maps, together with [23]Na concentration maps for comparison, was performed.

**Results:** ROI-based analyses of relaxation-weighted brain sodium concentration maps demonstrated increased sodium concentrations in the upper corticospinal tracts and in the frontal lobes in patients with ALS; no differences between ALS patients and controls were found in reference ROIs, where no involvement in ALS-associated neurodegeneration could be anticipated.

**Conclusion:** [23]NaR MRI mapped regional alterations within disease-relevant areas in ALS which correspond to the stages of the central nervous system (CNS) pathology, providing evidence that the technique is a potential biological marker of the cerebral neurodegenerative process in ALS.

*Keywords:* amyotrophic lateral sclerosis, corticospinal tract, frontal impairment, magnetic resonance imaging, neurodegenerative diseases, sodium imaging

Received: 26 April 2022; revised manuscript accepted: 1 June 2022.

Correspondence to:

**Jan Kassubek**
Department of Neurology, University of Ulm, Oberer Eselsberg 45, Ulm 89081, Germany

German Center for Neurodegenerative Diseases (DZNE), Ulm, Germany

**jan.kassubek@uni-ulm.de**

**Hans-Peter Müller**
Department of Neurology, University of Ulm, Ulm, Germany

**Armin M. Nagel**
Institute of Radiology, University Hospital Erlangen, Friedrich-Alexander-Universität Erlangen-Nürnberg (FAU), Erlangen, Germany

Division of Medical Physics in Radiology, German Cancer Research Center (DKFZ), Heidelberg, Germany

Department of Diagnostic and Interventional Radiology, University of Ulm, Ulm, Germany

Section for Experimental Radiology, University of Ulm Medical Center, Ulm, Germany

**Franziska Keidel**
Department of Diagnostic and Interventional Radiology, University of Ulm, Ulm, Germany

**Arthur Wunderlich**
Department of Diagnostic and Interventional Radiology, University of Ulm, Ulm, Germany

Section for Experimental Radiology, University of Ulm Medical Center, Ulm, Germany

## Introduction

Amyotrophic lateral sclerosis (ALS) is the most frequent adult-onset motor neuron disease, characterized by progressive pareses.[1,2] Despite the emphasis on the motor neurons, ALS has evolved to be regarded as a multisystem disorder,[3] given that it affects several brain regions in a distinctive propagation pattern.[4] In the clinical diagnostic processes, neuroimaging with magnetic resonance imaging (MRI) has an essential role in the exclusion of other etiologies of the clinical presentation.[5] In addition, MRI approaches with advanced postprocessing, focused on but not limited to diffusion-weighted imaging techniques, have been established as biological markers of the disease with reliable measures for monitoring

**Annemarie Hübers**
Department of Neurology, University of Ulm, Ulm, Germany

Department of Clinical Neurosciences, Geneva University Hospitals, Geneva, Switzerland

**Lena V. Gast**
Institute of Radiology, University Hospital Erlangen, Friedrich-Alexander-Universität Erlangen-Nürnberg (FAU), Erlangen, Germany

Department of Diagnostic and Interventional Radiology, University of Ulm, Ulm, Germany

**Albert C. Ludolph**
Department of Neurology, University of Ulm, Ulm, Germany German Center for Neurodegenerative Diseases (DZNE), Ulm, Germany

**Meinrad Beer**
Department of Diagnostic and Interventional Radiology, University of Ulm, Ulm, Germany

*These authors shared first authorship.

†These authors shared senior authorship.

disease progression and have greatly improved our understanding of its *in vivo* pathoanatomy.[6,7] In the search for features of diagnostic classifiers, the integration of multiparametric MRI including diffusion tensor imaging (DTI), volumetric, and texture data may be the best approach to generate a neuroimaging-based diagnostic tool for ALS,[8] also for multicenter studies.[9,10] In that context, the role of dedicated advanced MRI acquisition techniques has been more limited yet due to the specific and complex protocols which need a prospective study design, being $^1H$ magnetic resonance spectroscopy a typical example.[11] However, the potential of these techniques needs to be further taken use of. A range of processes shared with ALS impact ionic homeostasis including neuroinflammation and neurodegeneration by way of mitochondrial and sodium potassium pump ($Na^+/K^+$-ATPase) dysfunctions across the cell membrane, leading to intracellular sodium ($Na^+$) and subsequent calcium overload in patients.[12] These pathological processes could lead to homeostatic dysfunctions in motor regions and subsequent abnormal elevated sodium concentration in patients with ALS, while sodium dysbalance, in turn, could thus indicate early cellular dysfunction before degeneration of the cell.[13] As a promising advanced MRI approach, total tissue sodium concentration (which is associated with the viability of cells) can be assessed by $^{23}Na$ MRI.[14,15] The technique has been applied to study brain tissue, given that the $Na^+$ ion plays a crucial role in cell physiology as many conditions lead to changes in the average concentration of this element in cerebral tissue.[16] Grapperon and colleagues used $^{23}Na$ MRI to show that in patients with ALS, higher sodium concentration could be found in motor regions [bilateral precentral gyri, corticospinal tracts (CSTs), and corpus callosum].[12]

The $^{23}Na$ concentration data are a volume-weighted average of $^{23}Na$ assigned to the intra- and extracellular space, respectively. Thus, interstitial fluid, plasma, and cerebrospinal fluid (CSF) are attributed to the extracellular space; however, intracellular $^{23}Na$ might be more indicative of pathological processes. In contrast to the $^{23}Na$ concentration mapping, relaxation-based methods are a possibility to suppress $^{23}Na$ with a longitudinal relaxation time such as in CSF,[16] that way obtaining data with an increased weighting of intracellular space. Based on the differential sodium ion concentration between the intracellular and extracellular space, changes of the sodium ion concentration gradient point to pathological conditions, as investigated in neurodegenerative diseases like Huntington's disease.[17] Relaxation-weighted sodium MRI ($^{23}NaR$) enables a further differentiation of the total sodium signal by suppressing sodium signal that originates from long $T2^*$ compartments such as in fluids.[16] The aim of this study was to analyse the ALS-associated brain sodium homeostasis by applying $^{23}NaR$ MRI[16] to a group of participants with ALS in comparison to controls.

## Methods

### Subjects and patients

All participating patients and controls provided written informed consent for the study according to institutional guidelines. The study was approved by the Ethical Committee of the University of Ulm (reference #143/16).

The analysis included cross-sectional data from ALS patients ($N=17$) and controls ($N=10$; Table 1). All ALS patients underwent standardized clinical-neurological and routine laboratory examinations. The ALS patients (mean age $61.1 \pm 11.4$ years, m/f = 9/8) presented with a sporadic form of clinically definite or probable ALS according to the revised El Escorial diagnostic criteria.[18] Severity of physical symptoms, as measured with the revised ALS functional rating scale (ALS-FRS-R),[19] was $40 \pm 7$ (range 24–46). Disease duration was $17 \pm 13$ months. None of the ALS patients had a history of any other neurological or psychiatric disorders or other medical conditions. None of the patients had any contraindications against MRI scanning. A normal database of age-matched healthy controls (mean age $60.3 \pm 15.3$ years, m/f = 6/4, $p = 0.9$ compared to ALS) was used for comparison. None had a history of neurological or psychiatric disease. The total acquisition period of this study was 1 year (11/2018 to 11/2019).

### MRI acquisition

MRI scanning was performed on a 3.0 T Skyra (Siemens Medical, Erlangen, Germany) using a double-resonant ($^1H/^{23}Na$) quadrature birdcage coil (Rapid Biomedical GmbH, Rimpar, Germany). A double-echo, density-adapted 3D radial acquisition technique[20] was applied with the following parameters: $TE_1 = 0.3$ ms, $TE_2 = 25.0$ ms, repetition time $TR = 100$ ms, readout duration $T_{RO} = 20$ ms,

**Table 1.** Subjects' characteristics.

|  | ALS | controls | *p* |
|---|---|---|---|
| Male/female | 9/8 | 6/4 | 0.8 |
| Age/years, mean $\pm$ std. dev. (range) | 61 $\pm$ 11 (27 to 85) | 60 $\pm$ 15 (26 to 78) | 0.9 |
| Disease duration/months, mean $\pm$ std. dev. (range) | 17 $\pm$ 14 (2 to 40) | – | – |
| ALS-FRS-R, mean $\pm$ std. dev. (range) | 40 $\pm$ 7 (24 to 46) | – | – |
| ALS-FRS-R – slope/month, mean $\pm$ std. dev. (range) | −1.5 $\pm$ 3.7 (−0.1 to 15.5) | – | – |
| Site of onset (spinal/bulbar) | 17 / 0 | – | – |

ALS, amyotrophic lateral sclerosis; ALS-FRS-R, ALS functional rating scale.

nominal spatial resolution $4 \times 4 \times 4 \, mm^3$, flip angle: 90°, acquisition time: 13 min 20 s.

### MRI data analysis

The pre- and postprocessing was performed by use of the analysis software *Tensor Imaging and Fibre Tracking* (*TIFT*).[21]

### Stereotaxic normalization

Stereotaxic normalization was done by a rigid-brain-transformation to AC–PC-line, followed by a non-affine normalization according to landmarks. Intensity was normalized according to regression of sodium signal intensities derived from six chambers filled with 2% agarose gels with different NaCl-concentrations (25, 50, 75, 100, 125, and 150 mmol/L);[22] data processing is visualized in Figure 1.

### Relaxation weighting

According to a previously published protocol,[16] images with echo times $TE_1$ and $TE_2$ were subtracted using a weighted difference. The weighting factor $\exp[(TE_2-TE_1)/T_2^{*CSF}]$ was chosen such that sodium ions exhibiting relaxation properties like in CSF were fully suppressed. For each voxel, the difference intensity $I_D$ (representing the sodium concentration) was calculated according to

$$I_D\left(^{23}Na\right)=I\left(TE_1\right)-exp\left[\frac{TE_2-TE_1}{T_2^{*CSF}}\right]I\left(TE_2\right) \quad (1)$$

with $TE_1$ = 0.3 ms and $TE_2$ = 25.0 ms, and $T_2^{*CSF}$ = 56 ms, the weighting factor calculates as 1.554 (Figure 1).

The resulting difference maps were then smoothed with a Gaussian filter of FWHM 4 mm to obtain a good balance between sensitivity and specificity.

### ROI analyses

Based on the staging concept, ROI analysis was performed by locating spherical ROIs at predefined positions in the stereotaxically normalized difference maps, i.e. upper CST, frontal lobes, and basal ganglia. The corresponding anatomical localizations were selected in a hypothesis-guided approach according to results of previous MRI studies[9,23–25] where brain alterations have already been identified in accordance with the phosphorylated 43 kDa TAR DNA-binding protein (pTDP-43)-associated ALS propagation pattern.[4,26] As a reference region, an ROI was placed in the callosal area V where no involvement in ALS-associated neurodegeneration could be anticipated. Methodologically, the size of the ROIs was varied between 7 and 15 mm in order to investigate the dependence of differences between ALS patients and controls on ROI size. ROI positions were also varied by 5 mm in each spatial direction, that way detecting the optimum position at maximum differences between ALS patients and controls.

For comparison, ROI analysis in the upper CST, basal ganglia, and, as a reference, callosal area V was performed in $^{23}$Na concentration maps
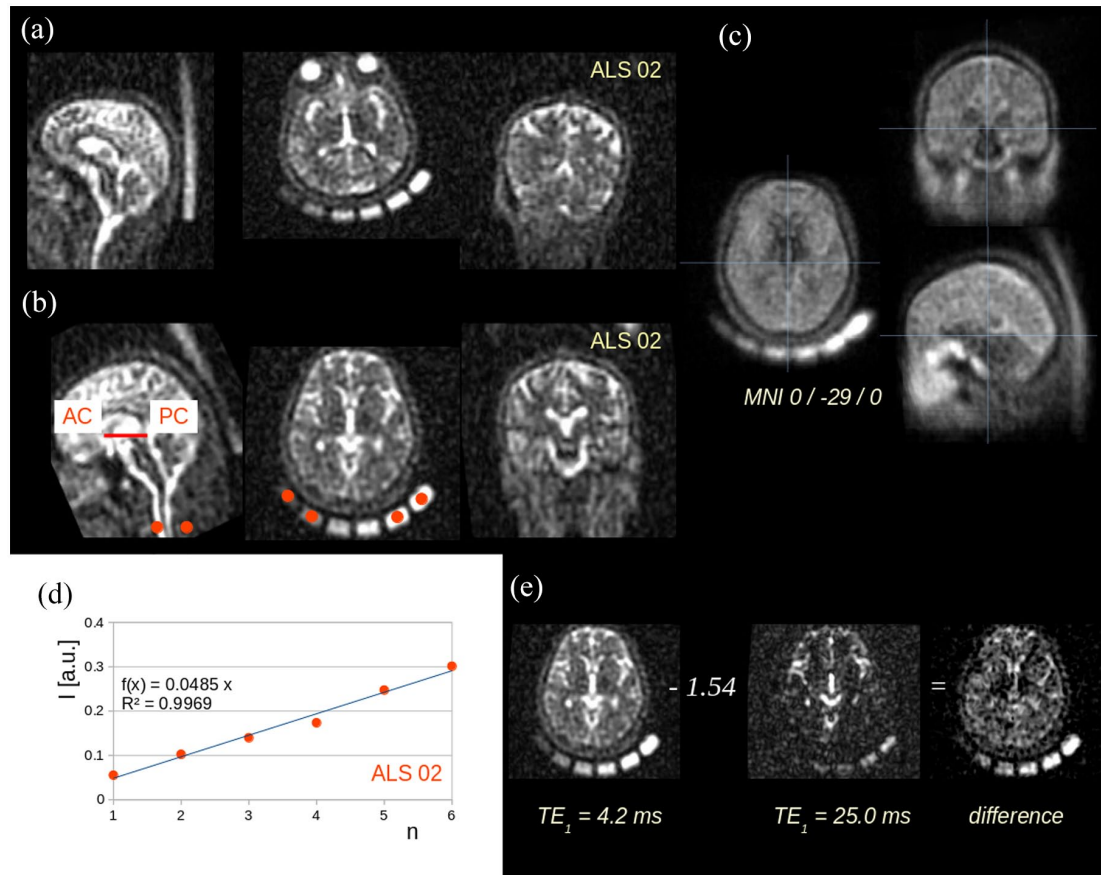
**Figure 1.** Data processing: example. (a) Originally recorded $^{23}$Na scan at TE1 (ALS patient 02) with six $^{23}$Na probes with slices in axial, coronar, and sagittal orientation. (b) The same data set after stereotaxic normalization to anterior commissure (AC) – posterior commissure (PC) orientation, note red ROIs located in the six $^{23}$Na probes. (c) Example for the quality of the normalization procedure: the template averaged from 27 subjects' $^{23}$NaR scans at $TE_1$. (d) Example for intensity normalization (ALS patient 02) according to regression analysis driven by ROI analysis of the six $^{23}$Na probes. (e) Relaxation weighting: images with echo times $TE_1$ and $TE_2$ were subtracted using a weighted difference of 1.54.

($TE_1 = 0.3$ ms). For correlation analyses, Spearman correlation was calculated to assess potential associations of regional $^{23}$Na accumulation ($^{23}$NaR MRI mapping as well as $^{23}$Na concentration mapping) with the clinical deficits (ALS-FRS-R) and disease duration, respectively.

## Results

To analyse sodium concentration alterations that are localized in the CST, i.e. related to ALS stage 1,[4] ROI locations in the upper CST were chosen. As additional ROI locations, we selected the frontal lobes and the basal ganglia, related to ALS stages 2 and 3, respectively;[4] furthermore, an ROI was placed in the callosal area V as a reference region for comparison where no ALS-associated affectation could be anticipated. In order to validate the choice of the ROIs, the variation both of the size of the ROIs and of the ROI localizations are summarized in Supplementary Figure 1.

A significant increase of sodium concentration in ALS patients at the group level was observed in the upper CST ($p < 0.0005$) and in the frontal lobes ($p < 0.01$) when compared to controls, as demonstrated in Figure 2. A trend for sodium concentration increase was observed in the basal ganglia ($p = 0.2$). No significant differences were observed in the callosal area V (reference region, $p = 0.9$). For comparison, the ROI analysis in $^{23}$Na concentration maps ($TE_1 = 0.3$ ms) revealed significantly increased $^{23}$Na accumulation in the upper CST (ALS patients: 44 mmol/L; controls: 41 mmol/L; $p < 0.05$) and in the frontal lobes
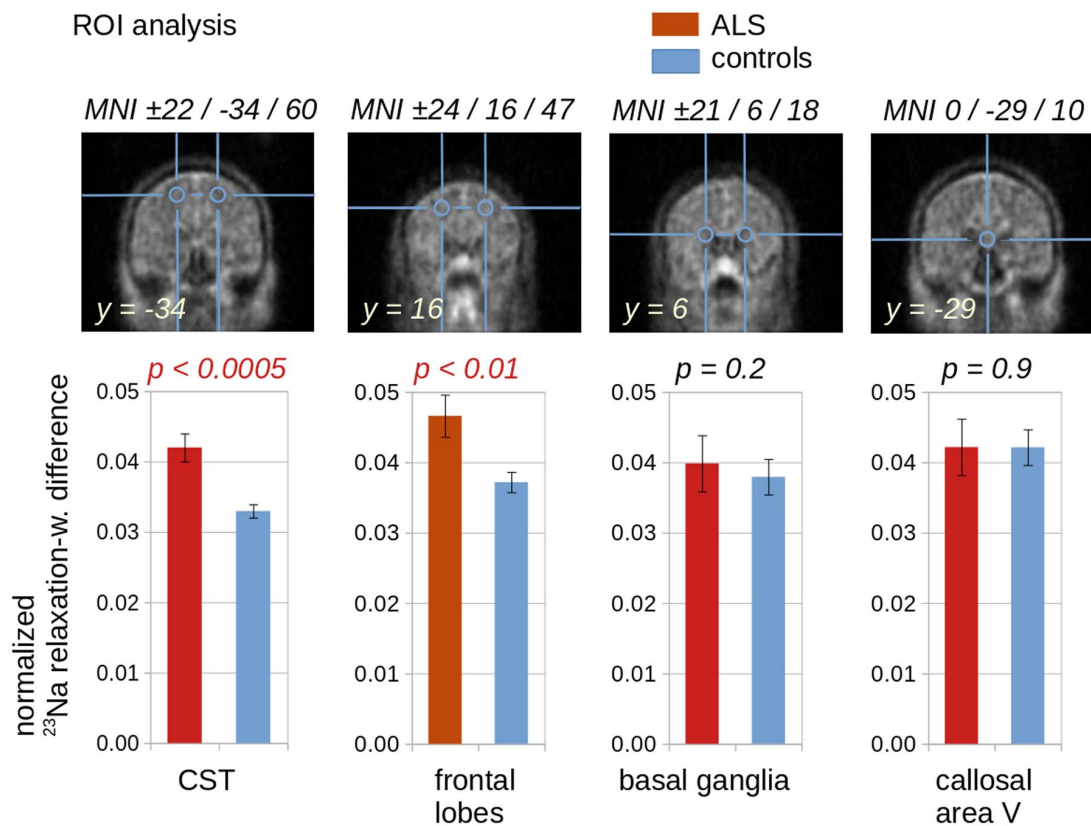
## ROI analysis



**Figure 2.** Results from ROI-based analysis of relaxation-weighted (relaxation-w.) difference. After filtering the normalized $^{23}$NaR difference maps with a Gaussian filter of FWHM 4 mm, spherical ROIs with a radius of 8 mm were placed in the upper corticospinal tract (CST) at MNI $\pm$ 22/-34/60 and in the frontal lobes at MNI $\pm$ 24/16/47, revealing significantly increased $^{23}$NaR in ALS patients at the group level. Analysis in basal ganglia (MNI $\pm$ 21/6/18) demonstrated a trend of increased $^{23}$NaR. The reference ROI in the callosal area V at MNI 0/-29/10 demonstrated no significant alterations. MNI – Montreal Neurological Institute coordinate frame.

(ALS patients: 43 mmol/L; controls: 39 mmol/L; $p < 0.05$); a trend of increased $^{23}$Na concentration was observed in the basal ganglia (ALS patients: 40 mmol/L, controls: 37 mmol/L; $p = 0.5$); no significant alterations were observed in the callosal area V (reference) (ALS patients: 43 mmol/L, controls: 44 mmol/L; $p = 0.8$; Supplementary Figure 2). Spearman correlation demonstrated no significant associations of the ROIs in the upper CST, frontal lobes, and basal ganglia with the ALS-FRS-R scores or with disease duration, respectively, neither for relaxation-weighted maps nor for concentration maps.

### Discussion

$^{23}$NaR MRI as an advanced metabolic imaging technique of the brain was shown to be capable to provide deeper insights into the pathophysiological mechanisms of tissue degeneration in ALS by localizing changes of cerebral tissue sodium concentration in ALS. The regional patterns of sodium homeostasis which could be identified included first, motor areas (i.e. upper CST) as the most prominent finding and second, frontal areas. As such, this topography of abnormal sodium concentration mirrored elements of the neuropathologically defined cerebral pTDP-43 distribution patterns of ALS, spreading from the motor neocortex downwards and then to frontal and last, parietal and anteromedial temporal lobes.[4,26] The involvement of primary motor cortices and CSTs in fact correspond to the core elements of the ALS pathoanatomy in the central nervous system, as has already been demonstrated *in vivo* by other MRI approaches like DTI.[27] $^{23}$NaR MRI as an advanced metabolic imaging technique has shown to be an improvement compared to $^{23}$Na concentration mapping; despite limited subject numbers, these results of the ROI analysis in $^{23}$Na concentration maps ($TE_1 = 0.3$ ms) and of the ROI analysis in $^{23}$NaR maps

are in accordance with previous results in sodium MRI.[12] Spearman correlation demonstrated no association of the ROIs in any of the investigated structures with ALS-FRS-R or with disease duration; here, the assumption is that a data sample of 17 patients might too low to perform this association analysis. The acquisition time of $^{23}$NaR MRI of less than 15 minutes can be regarded as an acceptable burden even for ALS patients in an advanced stage of disease. The regions which showed a common pattern of abnormally elevated sodium concentration correspond to the stages 1 and 2 of the central nervous system (CNS) pathology in ALS; the fact that the upper CST constituted the key area of the highest significant alterations is in line with other current studies in which the upper CST was identified as the region of the highest normalized importance across the most relevant imaging variables in computational models for the analysis of MRI data in ALS.[28] As such, findings in the current data may reflect the common pattern of CNS affectation found across the investigated ALS patients despite their heterogeneity of disease burden.

Thus, these findings support the hypothesis that elevated brain tissue sodium concentration as a measure of loss of cell integrity could be a potential marker of neurodegeneration processes; several pathophysiological processes involved in ALS, including mitochondrial dysfunction (as reported in ALS),[29] ionic disturbances, neuronal hyperexcitability, and neuroinflammation, could contribute to the altered sodium concentration observed in our and previous studies.[12] As such, the intraneuronal sodium overload may reflect both energy failure and axonal hyperexcitability as features of ALS.[12,30]

The application of relaxation-weighted $^{23}$Na MRI[16] offers the possibility to assess the fluid-suppressed sodium signal and to achieve a weighting towards the intracellular space. However, data quality control and analysis have to be thoroughly performed, given that the weighted subtraction image is more prone to susceptibility artefacts. The finding of regional sodium signal increase in $^{23}$NaR MRI (in contrast to signal reduction in $^{23}$NaR MRI, as it would be expected in association with local atrophy) might be due to the structure alterations and dysfunction of mitochondria which is regarded as a player in the pathogenesis of ALS, partially overlapping with other neurodegenerative diseases.[31] Although, the

ROI-based analysis was able to identify sodium increase in specific regions, the signal-to-noise ratio of the data sample of this study did not allow to detect sodium alteration along specific ALS-related tracts.[27]

This study had some limitations. First, the number of participants was limited and due to the novelty of the application of the $^{23}$NaR MRI technique to ALS, no estimation of the significance of the results could be performed and thus, no effect size/power calculation for study planning was possible. An increased sample size covering a larger spectrum of disease burden and also a longitudinal design could provide more insights in order to guide in the assessment of sources of heterogeneity at the individual patient level and in monitoring disease progression in the future. Second, different contributions to sodium signal such as intra- and extracellular sodium could not be distinguished, since a clear separation between intra- and extracellular sodium would require the use of paramagnetic shift reagents that cannot be applied in humans,[32] although relaxation-weighted imaging might result in a weighting towards the intracellular sodium.[16,33] Thus, our results are in accordance with an intraneuronal sodium increase. Third, although cognitive impairment is a well-established feature in ALS patients, a neuropsychological assessment was not part of the protocol in this methodological (proof-of-principle) study; we recommend the inclusion of dedicated neuropsychological data in future studies in $^{23}$Na-MRI in ALS. In the future, also other non-invasive techniques such as triple-quantum–filtered[14] or multiecho sodium MRI[34] or multipulse multicompartment quantification[35] might be exploited to further characterize the observed sodium concentration increase.

### Conclusion

In summary, this study provides evidence that $^{23}$NaR MRI depicts abnormal sodium concentration specifically in brain regions known to be particularly vulnerable in ALS and which correspond to the stages 1 and 2 of the pTDP-43 pathology of ALS. This mapping of tissue sodium concentration alterations could be a promising imaging biomarker to non-invasively analyse the regional cellular and metabolic integrity associated with neurodegeneration and might guide in monitoring the effects of therapeutic options which address e.g. mitochondrial dysfunction.

## Declarations

### Ethics approval and consent to participate
All participating patients and controls provided written informed consent for the study according to institutional guidelines. The study was approved by the Ethical Committee of the University of Ulm (reference #143/16).

### Consent for publication
All authors have agreed on publication.

### Author contributions
**Hans-Peter Müller:** Conceptualization; Formal analysis; Methodology; Writing – original draft.
**Armin M. Nagel:** Conceptualization; Investigation; Methodology; Writing – review & editing.
**Franziska Keidel:** Methodology; Writing – review & editing.
**Arthur Wunderlich:** Methodology; Writing – review & editing.
**Annemarie Hübers:** Methodology; Writing – review & editing.
**Lena V. Gast:** Methodology; Writing – review & editing.
**Albert C. Ludolph:** Investigation; Writing – review & editing.
**Meinrad Beer:** Conceptualization; Investigation; Writing – review & editing.
**Jan Kassubek:** Conceptualization; Investigation; Supervision; Writing – original draft.

### ORCID iDs
Armin M. Nagel (iD) https://orcid.org/0000-0003 -0948-1421
Annemarie Hübers (iD) https://orcid.org/0000-0002 -3088-0366
Jan Kassubek (iD) https://orcid.org/0000-0002-7106 -9270

### Conflict of interest statement
The authors declared the following potential conflicts of interest with respect to the research, authorship, and/or publication of this article: The authors declare that the research was conducted in the absence of any commercial or financial relationships that could be construed as a potential conflict of interest. An associate editor of *Therapeutic Advances in Chronic Disease* is an author of this paper; therefore, the peer-review process was managed by alternative members of the Board, and the Editor had no involvement in the decision-making process.

### Availability of data and materials
Data are available upon reasonable request. Reasonable data sharing requests are made in writing through Jan Kassubek (jan.kassubek@uni-ulm.de) and require a formal data sharing agreement. Data sharing agreements must include details on how the data will be stored, who will have access to the data and intended use of the data, and agreements as to the allocation of intellectual property.

### Supplemental material
Supplemental material for this article is available online.

### References

1. van Es MA, Hardiman O, Chio A, *et al.* Amyotrophic lateral sclerosis. *Lancet* 2017; 390: 2084–2098.

2. Goutman SA, Hardiman O, Al-Chalabi A, *et al.* Recent advances in the diagnosis and prognosis of amyotrophic lateral sclerosis. *Lancet Neurol* 2022; 21: 480–493.

3. Grossman M. Amyotrophic lateral sclerosis – a multisystem neurodegenerative disorder. *Nat Rev Neurol* 2019; 15: 5–6.

4. Braak H, Brettschneider J, Ludolph AC, *et al.* Amyotrophic lateral sclerosis – a model of corticofugal axonal spread. *Nat Rev Neurol* 2013; 9: 708–714.

5. Kassubek J and Müller HP. Advanced neuroimaging approaches in amyotrophic lateral sclerosis: refining the clinical diagnosis. *Expert Rev Neurother* 2020; 20: 237–249.

6. Chiò A, Pagani M, Agosta F, *et al.* Neuroimaging in amyotrophic lateral sclerosis: insights into structural and functional changes. *Lancet Neurol* 2014; 13: 1228–1240.

7. Kassubek J and Pagani M. Imaging in amyotrophic lateral sclerosis: MRI and PET. *Curr Opin Neurol* 2019; 32: 740–746.

8. Kocar TD, Müller HP, Ludolph AC, *et al.* Feature selection from magnetic resonance imaging data in ALS: a systematic review. *Ther Adv Chronic Dis* 2021; 12: 20406223211051002.

9. Müller HP, Turner MR, Grosskreutz J, *et al*. A large-scale multicentre cerebral diffusion tensor imaging study in amyotrophic lateral sclerosis. *J Neurol Neurosurg Psychiatry* 2016; 87: 570–579.

10. Filippi M, Agosta F, Grosskreutz J, *et al*. Progress towards a neuroimaging biomarker for amyotrophic lateral sclerosis. *Lancet Neurol* 2015; 14: 786–788.

11. Kalra S. Magnetic resonance spectroscopy in ALS. *Front Neurol* 2019; 10: 482.

12. Grapperon AM, Ridley B, Verschueren A, *et al*. Quantitative brain sodium MRI depicts corticospinal impairment in amyotrophic lateral sclerosis. *Radiology* 2019; 292: 422–428.

13. Boada FE, LaVerde G, Jungreis C, *et al*. Loss of cell ion homeostasis and cell viability in the brain: what sodium MRI can tell us. *Curr Top Dev Biol* 2005; 70: 77–101.

14. Madelin G, Lee JS, Regatte RR, *et al*. Sodium MRI: methods and applications. *Prog Nucl Magn Reson Spectrosc* 2014; 79: 14–47.

15. Huhn K, Engelhorn T, Linker RA, *et al*. Potential of sodium MRI as a biomarker for neurodegeneration and neuroinflammation in multiple sclerosis. *Front Neurol* 2019; 10: 84.

16. Nagel AM, Bock M, Hartmann C, *et al*. The potential of relaxation-weighted sodium magnetic resonance imaging as demonstrated on brain tumors. *Invest Radiol* 2011; 46: 539–547.

17. Reetz K, Romanzetti S, Dogan I, *et al*. Increased brain tissue sodium concentration in Huntington's Disease – a sodium imaging study at 4 T. *NeuroImage* 2012; 63: 517–524.

18. Brooks BR, Miller RG, Swash M, *et al*. El Escorial revisited: revised criteria for the diagnosis of amyotrophic lateral sclerosis. *Amyotroph Lateral Scler Other Motor Neuron Disord* 2000; 1: 293–299.

19. Cedarbaum JM, Stambler N, Malta E, *et al*. The ALSFRS-R: a revised ALS functional rating scale that incorporates assessments of respiratory function. BDNF ALS Study Group (Phase III). *J Neurol Sci* 1999; 169: 13–21.

20. Nagel AM, Laun FB, Weber MA, *et al*. Sodium MRI using a density-adapted 3D radial acquisition technique. *Magn Reson Med* 2009; 62: 1565–1573.

21. Müller HP, Unrath A, Ludolph AC, *et al*. Preservation of diffusion tensor properties during spatial normalization by use of tensor imaging and fibre tracking on a normal brain database. *Phys Med Biol* 2007; 52: N99–N109.

22. Mirkes CC, Hoffmann J, Shajan G, *et al*. High-resolution quantitative sodium imaging at 9.4 Tesla. *Magn Reson Med* 2015; 73: 342–351.

23. Kassubek J, Müller HP, Del Tredici K, *et al*. Diffusion tensor imaging analysis of sequential spreading of disease in amyotrophic lateral sclerosis confirms patterns of TDP-43 pathology. *Brain* 2014; 137: 1733–1740.

24. Kalra S, Müller HP, Ishaque A, *et al*. A prospective harmonized multicenter DTI study of cerebral white matter degeneration in ALS. *Neurology* 2020; 95: e943–e952.

25. Bede P, Elamin M, Byrne S, *et al*. Basal ganglia involvement in amyotrophic lateral sclerosis. *Neurology* 2013; 81: 2107–2115.

26. Brettschneider J, Del Tredici K, Toledo JB, *et al*. Stages of pTDP-43 pathology in amyotrophic lateral sclerosis. *Ann Neurol* 2013; 74: 20–38.

27. Kassubek J, Müller HP, Del Tredici K, *et al*. Imaging the pathoanatomy of amyotrophic lateral sclerosis in vivo: targeting a propagation-based biological marker. *J Neurol Neurosurg Psychiatry* 2018; 89: 374–381.

28. Bede P, Murad A and Hardiman O. Pathological neural networks and artificial neural networks in ALS: diagnostic classification based on pathognomonic neuroimaging features. *J Neurol* 2022; 269: 2440–2452.

29. Turner MR, Bowser R, Bruijn L, *et al*. Mechanisms, models and biomarkers in amyotrophic lateral sclerosis. *Amyotroph Lateral Scler Frontotemporal Degener* 2013; 14(Suppl. 1): 19–32.

30. Vucic S and Kiernan MC. Axonal excitability properties in amyotrophic lateral sclerosis. *Clin Neurophysiol* 2006; 117: 1458–1466.

31. Jankovic M, Novakovic I, Gamil Anwar Dawod P, *et al*. Current concepts on genetic aspects of mitochondrial dysfunction in amyotrophic lateral sclerosis. *Int J Mol Sci* 2021; 22: 9832.

32. Kline RP, Wu EX, Petrylak DP, *et al*. Rapid in vivo monitoring of chemotherapeutic response using weighted sodium magnetic resonance imaging. *Clin Cancer Res* 2000; 6: 2146–2156.

33. Konstandin S and Nagel AM. Measurement techniques for magnetic resonance imaging of fast relaxing nuclei. *MAGMA* 2014; 27: 5–19.

34. Ridley B, Nagel AM, Bydder M, *et al*. Distribution of brain sodium long and short relaxation times and concentrations: a multi-echo ultra-high field 23Na MRI study. *Sci Rep* 2018; 8: 4357.

35. Gilles A, Nagel AM and Madelin G. Multipulse sodium magnetic resonance imaging for multicompartment quantification: proof-of-concept. *Sci Rep* 2017; 7: 17435.

Visit SAGE journals online
journals.sagepub.com/
home/taj

SAGE journals

8

journals.sagepub.com/home/taj